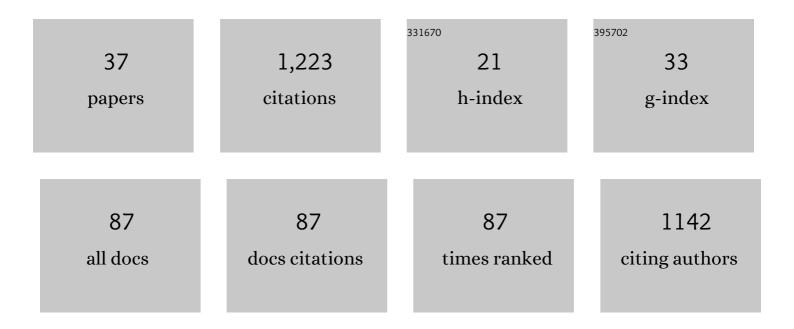


List of Publications by Year in descending order

Source: https://exaly.com/author-pdf/1041744/publications.pdf Version: 2024-02-01



Προ Εριέ ΑΫ

#	Article	IF	CITATIONS
1	Evolution of observed ozone, trace gases, and meteorological variables over Arrival Heights, Antarctica (77.8°S, 166.7°E) during the 2019 Antarctic stratospheric sudden warming. Tellus, Series B: Chemical and Physical Meteorology, 2022, 73, 1933783.	1.6	3
2	Enhancing MAX-DOAS atmospheric state retrievals by multispectral polarimetry – studies using synthetic data. Atmospheric Measurement Techniques, 2022, 15, 2077-2098.	3.1	2
3	Ground-based validation of the MetOp-A and MetOp-B GOME-2 OClO measurements. Atmospheric Measurement Techniques, 2022, 15, 3439-3463.	3.1	Ο
4	Time-dependent 3D simulations of tropospheric ozone depletion events in the Arctic spring using the Weather Research and Forecasting model coupled with Chemistry (WRF-Chem). Atmospheric Chemistry and Physics, 2021, 21, 7611-7638.	4.9	13
5	Intercomparison of MAX-DOAS vertical profile retrieval algorithms: studies on field data from the CINDI-2 campaign. Atmospheric Measurement Techniques, 2021, 14, 1-35.	3.1	32
6	Retrieval algorithm for OClO from TROPOMI (TROPOspheric Monitoring Instrument) by differential optical absorption spectroscopy. Atmospheric Measurement Techniques, 2021, 14, 7595-7625.	3.1	2
7	Validation of MAX-DOAS retrievals of aerosol extinction, SO ₂ , and NO ₂ through comparison with lidar, sun photometer, active DOAS, and aircraft measurements in the Athabasca oil sands region. Atmospheric Measurement Techniques, 2020, 13, 1129-1155.	3.1	4
8	Evaluating different methods for elevation calibration of MAX-DOAS (Multi AXis Differential Optical) Tj ETQq0 0 Techniques, 2020, 13, 685-712.	0 rgBT /0 3.1	verlock 10 Tf 11
9	Intercomparison of NO ₂ , O ₄ , O ₃ and HCHO slant column measurements by MAX-DOAS and zenith-sky UV–visible spectrometers during CINDI-2. Atmospheric Measurement Techniques. 2020. 13. 2169-2208.	3.1	52
10	Inter-comparison of MAX-DOAS measurements of tropospheric HONO slant column densities and vertical profiles during the CINDI-2 campaign. Atmospheric Measurement Techniques, 2020, 13, 5087-5116.	3.1	18
11	Validation of tropospheric NO ₂ column measurements of GOME-2A and OMI using MAX-DOAS and direct sun network observations. Atmospheric Measurement Techniques, 2020, 13, 6141-6174.	3.1	31
12	Recent improvements of long-path DOAS measurements: impact on accuracy and stability of short-term and automated long-term observations. Atmospheric Measurement Techniques, 2019, 12, 4149-4169.	3.1	7
13	Intercomparison of MAX-DOAS vertical profile retrieval algorithms: studies using synthetic data. Atmospheric Measurement Techniques, 2019, 12, 2155-2181.	3.1	34
14	Is a scaling factor required to obtain closure between measured and modelled atmospheric O ₄ absorptions? An assessment of uncertainties of measurements and radiative transfer simulations for 2 selected days during the MAD-CAT campaign. Atmospheric Measurement Techniques, 2019, 12, 2745-2817.	3.1	22
15	Detection of O ₄ absorption around 328 and 419†nm in measured atmospheric absorption spectra. Atmospheric Chemistry and Physics, 2018, 18, 1671-1683.	4.9	7
16	Springtime Bromine Activation over Coastal and Inland Arctic Snowpacks. ACS Earth and Space Chemistry, 2018, 2, 1075-1086.	2.7	22
17	Daytime HONO, NO ₂ and aerosol distributions from MAX-DOAS observations in Melbourne. Atmospheric Chemistry and Physics, 2018, 18, 13969-13985.	4.9	34
18	Observations of bromine monoxide transport in the Arctic sustained on aerosol particles. Atmospheric Chemistry and Physics, 2017, 17, 7567-7579.	4.9	44

Udo Frieß

#	Article	IF	CITATIONS
19	Horizontal and vertical structure of reactive bromine events probed by bromine monoxide MAX-DOAS. Atmospheric Chemistry and Physics, 2017, 17, 9291-9309.	4.9	27
20	Detection of water vapour absorption around 363 nm in measured atmospheric absorption spectra and its effect on DOAS evaluations. Atmospheric Chemistry and Physics, 2017, 17, 1271-1295.	4.9	36
21	MAX-DOAS retrieval of aerosol extinction properties in Madrid, Spain. Atmospheric Measurement Techniques, 2016, 9, 5089-5101.	3.1	30
22	Intercomparison of aerosol extinction profiles retrieved from MAX-DOAS measurements. Atmospheric Measurement Techniques, 2016, 9, 3205-3222.	3.1	53
23	Biogenic halocarbons from the Peruvian upwelling region as tropospheric halogen source. Atmospheric Chemistry and Physics, 2016, 16, 12219-12237.	4.9	22
24	The role of open lead interactions in atmospheric ozone variability between Arctic coastal and inland sites. Elementa, 2016, 4, .	3.2	6
25	Dependence of the vertical distribution of bromine monoxide in the lower troposphere on meteorological factors such as wind speed and stability. Atmospheric Chemistry and Physics, 2015, 15, 2119-2137.	4.9	41
26	Vertical distribution of BrO in the boundary layer at the Dead Sea. Environmental Chemistry, 2015, 12, 438.	1.5	16
27	The impact of vibrational Raman scattering of air on DOAS measurements of atmospheric trace gases. Atmospheric Measurement Techniques, 2015, 8, 3767-3787.	3.1	27
28	On the relative absorption strengths of water vapour in the blue wavelength range. Atmospheric Measurement Techniques, 2015, 8, 4329-4346.	3.1	30
29	Cloud detection and classification based on MAX-DOAS observations. Atmospheric Measurement Techniques, 2014, 7, 1289-1320.	3.1	63
30	The Heidelberg Airborne Imaging DOAS Instrument (HAIDI) – a novel imaging DOAS device for 2-D and 3-D imaging of trace gases and aerosols. Atmospheric Measurement Techniques, 2014, 7, 3459-3485.	3.1	33
31	Glyoxal observations in the global marine boundary layer. Journal of Geophysical Research D: Atmospheres, 2014, 119, 6160-6169.	3.3	38
32	CARIBIC DOAS observations of nitrous acid and formaldehyde in a large convective cloud. Atmospheric Chemistry and Physics, 2014, 14, 6621-6642.	4.9	8
33	MAX-DOAS formaldehyde slant column measurements during CINDI: intercomparison and analysis improvement. Atmospheric Measurement Techniques, 2013, 6, 167-185.	3.1	78
34	lodine monoxide in the Western Pacific marine boundary layer. Atmospheric Chemistry and Physics, 2013, 13, 3363-3378.	4.9	66
35	Atmospheric mercury over sea ice during the OASIS-2009 campaign. Atmospheric Chemistry and Physics, 2013, 13, 7007-7021.	4.9	42
36	Ozone dynamics and snowâ€atmosphere exchanges during ozone depletion events at Barrow, Alaska. Journal of Geophysical Research, 2012, 117, .	3.3	52

#	Article	IF	CITATIONS
37	The Monte Carlo atmospheric radiative transfer model McArtim: Introduction and validation of Jacobians and 3D features. Journal of Quantitative Spectroscopy and Radiative Transfer, 2011, 112, 1119-1137.	2.3	174